Journal of Solid and Fluid Mechanics (JSFM), 13(3): 1-6, 2023

Shahrood University of Technology

Journal of Solid and Fluid Mechanics (JSFM)

DOI: 10.22044/JSFM.2023.12483.3677

Manufacturing Engineering of Iran

Characterization of Flow and Hardening Parameters of 1100 Aluminium Alloy by Combining Nanoindentation Test and Crystal Plasticity Finite Element Simulation

Ali Aghabalaeivahid[1], Vali Alimirzaloo[2]

[1] Ph.D. Student, Department of Mechanical Engineering, Faculty of Engineering, Urmia University, Urmia, Iran
[2] Assoc. Prof., Department of Mechanical Engineering, Faculty of Engineering, Urmia University, Urmia, Iran

*Corresponding author: aliaghabalaeivahid@gmail.com

Received: 12/10/2022 Revised: 04/05/2023 Accepted: 07/31/2023

Abstract

The mechanical response of crystalline materials is affected by the flow and hardening of dislocations; that to describe them as a material model in finite element calculations, the flow and hardening parameters are implemented in the crystal plasticity code. In the present study, flow and hardening parameters for 1100 aluminium alloy were characterized by combining the experimental nanoindentation test and 3D crystal plasticity finite element simulations. Extracted parameters were validated by comparing the stress-strain curves of the experimental uniaxial tensile test and simulation of 3D crystal plasticity finite element on single crystal and polycrystal models. Also, the effect of the friction coefficient in determining the flow and hardening parameters was discussed. The results of this study showed that (i) parameters of initial yield stress, reference shear strain rate, and saturation stress, respectively, had the highest positive correlation with the maximum load; (ii) the load-displacement curve obtained from the simulation of the nanoindentation test using the characterized parameters has a relative error of 0.50% compared to the experimental nanoindentation test at the maximum indentation depth; (iii) The characterized parameters significantly can estimate the yield stress and ultimate tensile strength with a relative error of 2.60% and 0.20% for the single crystal model and 10.18% and 12.44% for the polycrystal model, respectively. However, while accurately modeling the yield zone in the polycrystal model, the accuracy of the characterized parameters is affected by the grain boundary orientation.

Keywords: Flow and Hardening Parameters; Finite Element Method; Crystal Plasticity; Nanoindentation; 1100 Aluminium Alloy.

1. Introduction

Polycrystalline materials exhibit distinct behavior at the micro and meso scales compared to the macro scale, making it challenging to characterize their flow and hardening parameters with conventional tests like tensile and pressure tests. One approach to solving this problem is to model the governing physical laws on a microscopic scale and generalize the results to the entire material [1]. The crystal plasticity model, which considers the inherent anisotropy of elastic and plastic properties at the meso scale, has successfully predicted the mechanical response of crystalline materials. So far, researchers have widely used the approach of comparing numerical simulations from macro to nanoscales to characterize constitutive parameter values for predicting the behavior of crystalline materials [2, 3].

This study innovatively combines experimental nanoindentation tests and 3D crystal plasticity finite element (3D CPFE) simulations to characterize the flow and hardening parameters of 1100 aluminum alloy, taking into account reflection symmetry in each rotational section in the [001] and [110] crystal directions and validating the determined parameters by 3D CPFE simulation of uniaxial tensile tests on single crystal and polycrystal models.

2. 3D crystal plasticity finite element simulation

This research uses the 3D CPFE method to simulate the nanoindentation test on a single crystal model and the uniaxial tensile test on single crystal and polycrystal models of 1100 aluminum alloy based on the experimental test conditions of Ref. [4]. The crystal plasticity theory principles used in this research are based on the studies of Rice [5], Peirce [6], Asaro [7], and the hardening law of Peirce et al. [8]. The modeling process of the nanoindentation test was simplified by using one-eighth of the sample due to the reflection symmetry in each rotational section in the [001] and [110] crystal directions. The boundary conditions in simulating the 3D CPFE of the nanoindentation test were applied as follows: The bottom surface nodes were restricted to the indentation direction but allowed to move freely in the direction perpendicular to the direction the indenter was moving. Symmetric planes

only moved within their planes. The vertical displacement of the indenter was set as indentation depth up to the depth reached by the experiment [4].

A uniaxial tensile test was used to validate the characterized flow and hardness parameters. To simulate the uniaxial tensile test of the polycrystal model, the representative volume element (RVE) of the 3D polycrystal microstructure of 1100 aluminum alloy with dimensions of 0.03 × 0.03 mm and 110 grains were produced by Dream.3D software. The number of polycrystal model elements is equal to 27000 elements. In the 3D CPFE simulation of the uniaxial tensile test on single crystal model, the dimensions of the single crystal model were considered equal to the average grain size produced in the polycrystal model. Thus, the dimensions of the single crystal model were 0.0036 × 0.0036 × 0.0036 mm, and the number of elements was 1000 elements. To apply the boundary conditions, both models were constrained in the planes of symmetry in three main directions. Finally, the created models were subjected to uniaxial tensile simulation with a strain rate of 0.001 S^{-1} according to Ref. [4] in the [001] direction, corresponding with the direction used in the nanoindentation test simulation.

In all three simulations, the slip system set [110] (111) with 12 different slip systems was considered. For the simulations of the nanoindentation test and uniaxial tensile test, the mesh types used were C3D8R and C3D6 for the former and C3D8R for the latter.

3. Parameters and levels of the experiment

In this research, the flow and hardening parameters of 1100 aluminum alloy are characterized by determining a set of material properties that better match the simulation results with the target experimental data; For this purpose, the method of one factor at a time (OFAT), in which the effect of each of the flow and hardening parameters can be observed by changing only one parameter for each simulation has been used.

In Table 1, the levels of the parameters are listed. The value of the elasticity modulus and Poisson's ratio based on the experimental data [9] was considered 79.84 GPa and 0.33, respectively.

Table 1. Flow and hardening parameters and levels were selected in the experiment.

Parameters	Level 1	Level 2	Level 3
n	8	12	20
$\dot{\gamma}_0^{(\alpha)}$ (S^{-1})	0.0001	0.001	0.01
h_0 (MPa)	120	240	360
τ_s (MPa)	105	210	315
τ_0 (MPa)	90	180	270
q	1	1.4	2
FC	0	0.3	0.6

4. Results and Discussion

4.1. Mesh sensitivity

To simulate the nanoindentation test, three different element sizes were used in the indentation zone to assess mesh sensitivity: 11 nm (mesh-1), 5.5 nm (mesh-2), and 3.6 nm (mesh-3). Mesh-1 had the largest element size, with 9600 elements, and resulted in more significant oscillations in the load-displacement curve due to shape instability under contact load (Figure 1(a)). Although the contact surface-displacement curves of mesh-2 (44200 elements) and mesh-3 (126000 elements) are not completely consistent with each other (Figure 1(b)), the effect of the oscillations in the load-displacement curve reduced quickly; Thus, Mesh-2 was chosen for all nanoindentation test simulations.

For the 3D CPFE simulation of the uniaxial tensile test on the single crystal model, there was no mesh sensitivity as deformation occurred homogeneously in the [001] crystal direction [10]. The 3D CPFE simulation of uniaxial tensile test on polycrystal model consists of 63 elements per grain and a normal size distribution of 110 RVE grains, selected for accuracy and computational speed based on Ref. [10].

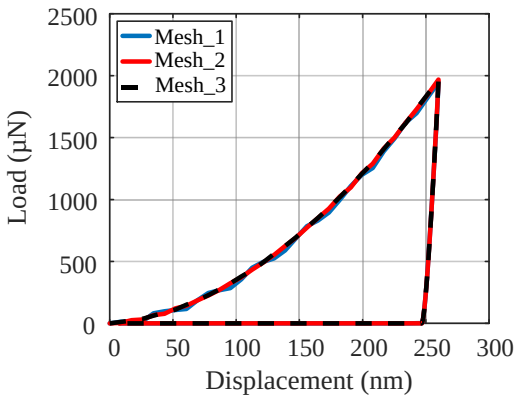

(a)

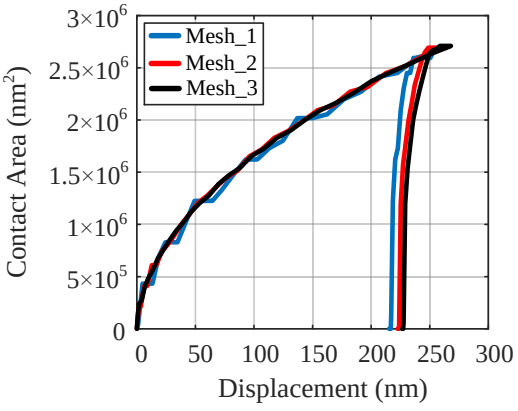

(b)

Figure 1. Mesh convergence test results in (a) load-displacement curves and (b) contact surface-displacement curves.

4.2. Simplified model's results accuracy

To ensure the accuracy of the simplified model's results, a numerical verification test was conducted on an angular section of the cylindrical region at the center of the indentation axis using symmetric boundary conditions. Simulations were performed using the simplified model, one-eighth of the full cylindrical model, and the full cylindrical model. A good match was observed between the load-displacement curves for both sets of boundary conditions, with an average relative error of 0.0004% and a maximum relative error of 0.14%. So that the surface profile caused by nanoindentation on the (001) plane of the full cylindrical model displayed true simplification in [001] and [110] crystal directions, with piling-up apparent due to reflection symmetry in each rotation section (Figure 2). Consequently, the simplified model was used for all nanoindentation test simulations to increase calculation speed.

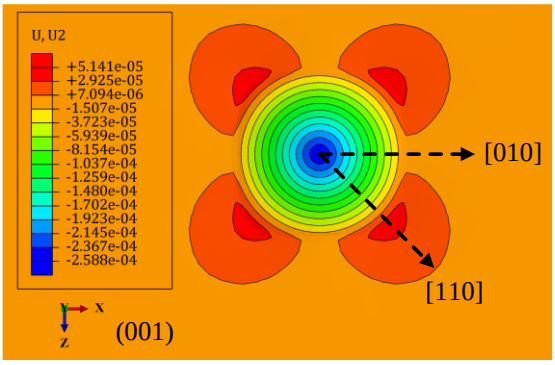

Figure 2. Surface profile caused by nanoindentation at the end of loading on the (001) plane of full cylindrical model.

4.3. Characterization of flow and hardening parameters

In this section, the approach of determining each of the flow and hardening parameters of 1100 aluminum alloy by combining the nanoindentation test and the 3D CPFE simulation is explained. Figure 3 shows the effect of each parameter according to the values mentioned in Table 1 on the load-displacement curves. The strain rate sensitivity n, initial hardening modulus h_0, saturation stress τ_s, and latent hardening parameter q all significantly do not affect the load-displacement curves. For example, by changes in the strain rate sensitivity n from 8 to 12 or 20, or the initial hardening modulus h_0 from 120 MPa to 240 and 360 MPa, no significant change is seen. The reference shear strain rate $\dot{\gamma}_0^{(\alpha)}$, and initial critical resolved shear stress τ_0 are the most dominant parameters affecting the material's properties. Regarding the friction coefficient, it can be seen that the indentation depth is not affected by the friction coefficient; Therefore, the indentation depth for all three surfaces is constant and independent of the friction coefficient. Additionally, the load-displacement curves have similar oscillation ranges. Consequently, the simulated load-displacement curves are not affected by the friction coefficient on the contact surface between the nano-indenter and the sample. This conclusion aligns with findings from other studies. [11, 12]. Accordingly, by comparing the simulated and experimental load-displacement curves, the values of the flow and hardening parameters for 1100 aluminum alloy were characterized and are provided in Table 2.

Table 2. Characterized flow and hardening parameters for 1100 aluminum alloy.

Parameters	Symbol	Value
Strain rate sensitivity	n	8
Reference shear strain rate	$\dot{\gamma}_0^{(\alpha)}$ (S^{-1})	0.001
Initial hardening modulus	h_0 (MPa)	120
Saturation stress	τ_s (MPa)	105
Initial critical resolved shear stress	τ_0 (MPa)	90
Latent hardening parameter	q	1
Friction coefficient	FC	0

3D CPFE simulation of nanoindentation test using characterized flow and hardening parameters for 1100 aluminum alloy in Table 2 was performed again, and the resulting load-displacement curve is shown in Figure 4. As shown in Figure 4, the simulated load-displacement curve by the characterized parameters agrees with the experimental load-displacement curve. So that the maximum indentation depth in the simulation of the nanoindentation test with identified parameters is 260 nm with the application of an indentation load of 1968.5 µN with a relative error of 0.50% compared to the experimental nanoindentation test in which the maximum indentation depth is 260 nm with the indentation load of 1949 µN.

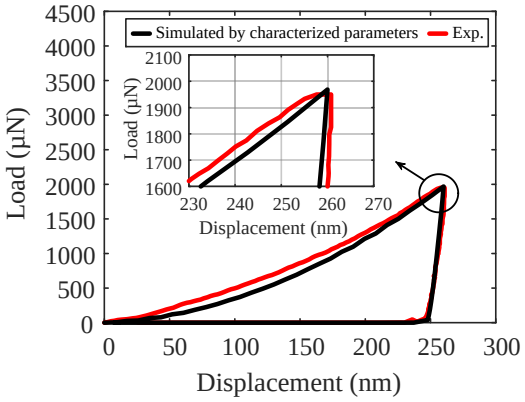

Figure 4. Simulation load-displacement curve by the characterized parameters and comparison with the experimental load-displacement curve of Ref. [4].

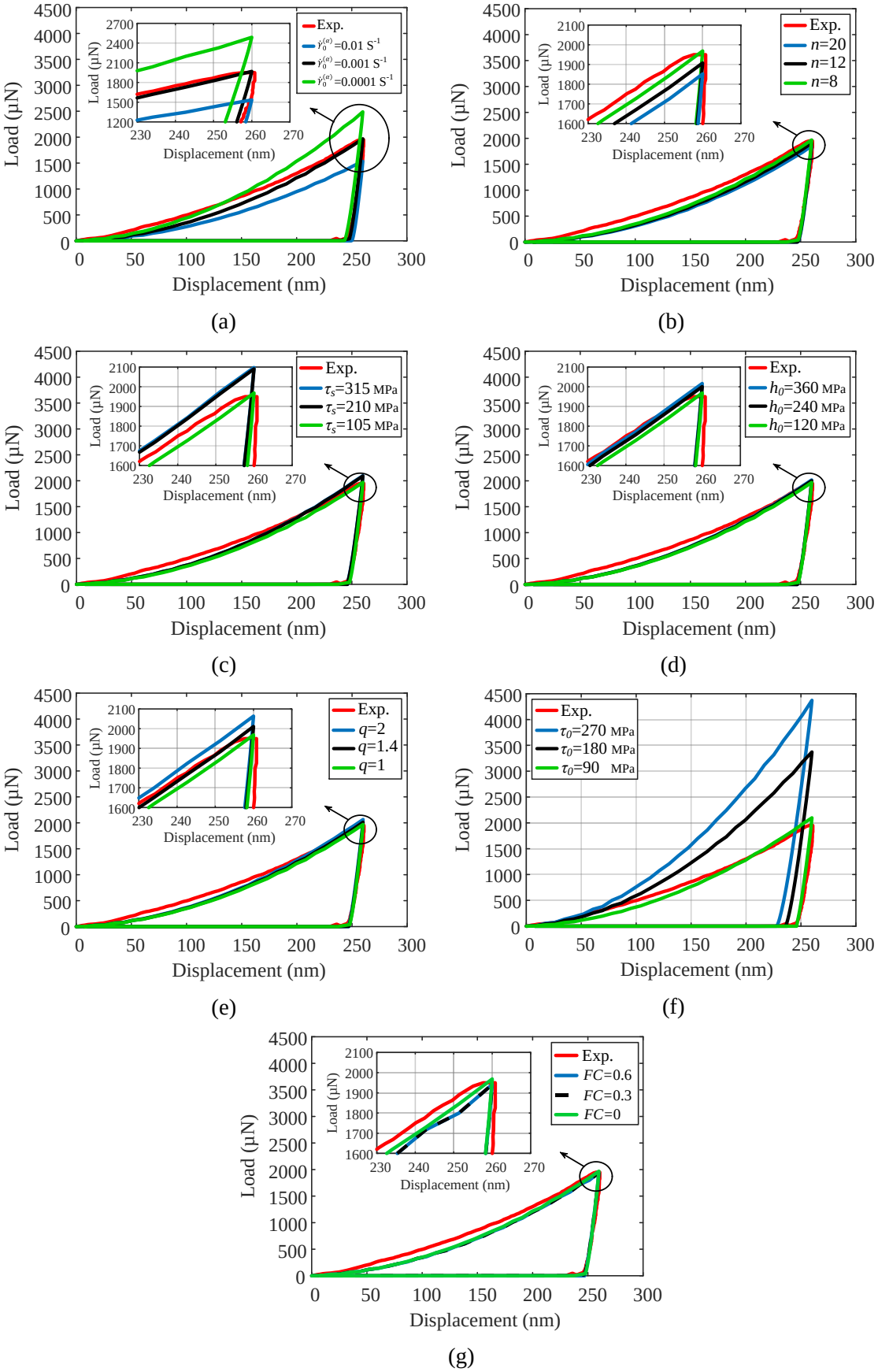

Figure 3. Effect of (a) reference shear strain rate, (b) strain rate sensitivity, (c) saturation stress, (d) initial hardening modulus, (e) latent hardening parameter, (f) initial critical resolved shear stress, and (g) friction coefficient on the simulated load-displacement curves and comparison with the experimental load-displacement curve of Ref. [4].

4.4. Validating the characterized parameters

The purpose of validating the characterized parameters is to link the scale from the single crystal in the nanoindentation test to the related technical dimension in the uniaxial tensile test while considering the heterogeneous characteristics of the polycrystal. The experimental and simulation stress-strain curves in Figure 5(a) confirm the accuracy of the characterized parameters in the single crystal model for strains greater than 0.005, accurately estimating yield stress (YS) and ultimate tensile strength (UTS) with a relative error of 2.60% and 0.20%, respectively. Homogeneous deformation in the [001] crystal direction has caused sudden yielding in the elastic region of the single crystal model curve, with slight deviations at low strains [10]. Despite these deviations at low strains, the characterized parameters are reliable in predicting macroscopic stresses compared to the experimental curve, indicating consistent energy consumption during aluminum alloy deformation at macro and single crystal scales. Specifically, it can be concluded that the hardening mechanisms of 1100 aluminum alloy are the same at the macro scale and in single crystals that undergo deformation in the [110] (111) slip system assembly. These results are consistent with Howe and Elbaum's results [13].

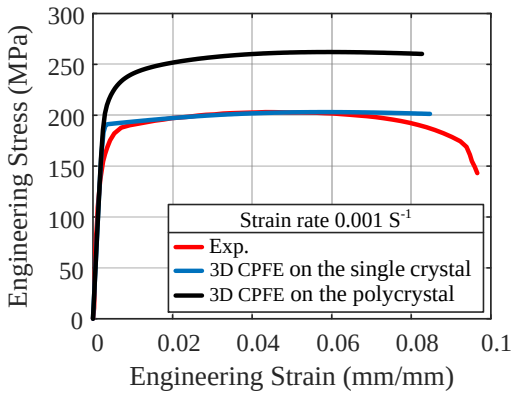

(a)

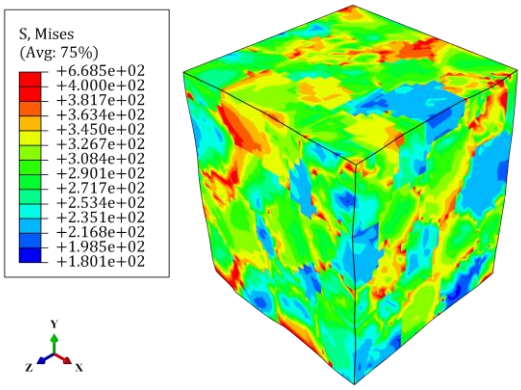

(b)

Figure 5. (a) Engineering stress-strain curves of Ref. [4] and 3D CPFE uniaxial tensile test of 1100 aluminum alloy; (b) Mises stress contour of uniaxial tensile test of polycrystal model.

In the polycrystal model, despite the stress-strain curve agreeing with the experimental curve, the accuracy of the stress-strain curve is affected by stress concentration and local hardening occurring in the grain boundaries due to changes in crystal directions. Thus, the relative error of YS and UTS in the polycrystal model is 10.18% and 12.44%, respectively, with 7% of the errors related to the total number of elements and number of elements per grain and the rest due to neglecting grain boundaries and other parameters.

5. Conclusions

This paper combines experimental nanoindentation tests and 3D CPFE simulations to characterize the flow and hardening parameters of 1100 aluminum alloy. The parameters consider reflection symmetry in each rotational section in the [001] and [110] crystal directions and investigate the friction coefficient's influence. The characterized parameters are verified through 3D CPFE simulation of uniaxial tensile test on single crystal and polycrystal models. The research findings demonstrated that:

1) Parameters of initial critical resolved shear stress, reference shear strain rate, and saturation stress have the highest positive correlation with the maximum load, respectively.
2) The combination of nanoindentation test and 3D CPFE simulation accurately characterized the flow and hardening parameters of 1100 aluminum alloy. The load-displacement curve obtained from the simulation has a relative error of 0.50% at maximum indentation depth compared to the experimental nanoindentation test.
3) The characterized flow and hardening parameters of 1100 aluminum alloy significantly improved the ability to estimate the YS and UTS with a relative error of 2.60% and 0.20%, respectively, in the 3D CPFE simulation of uniaxial tensile test on single crystal model. The result indicates that energies consumed during the deformation and hardening mechanisms of 1100 aluminum alloy are the same in single crystal and macro scales.
4) While accurately modeling the yield zone in the 3D CPFE simulation of uniaxial tensile test on polycrystal model, the accuracy of characterized parameters in this model is affected by grain boundary orientation. However, it can still estimate the YS and UTS with a relative error of 10.18% and 12.44%, respectively.
5) The presented simulation model captures the main features of the nanoindentation test, such that resistance force on the indenter increases with indentation depth and decreases quickly upon the indenter's return and exit. Also, the simulated load-displacement curve matches well with the experimental load-displacement curve in loading and unloading during the nanoindentation test.

6. References

[1] Phillips, R., Crystals, defects and microstructures: modeling across scales. 2001: *Cambridge University Press.*

[2] Liu, M., et al., A combined experimental-numerical approach for determining mechanical properties of aluminum subjects to nanoindentation. *Scientific reports*, 2015. 5(1): p. 1-16.

[3] Aghabalaeivahid, A. and M. Shalvandi, Microstructure-based crystal plasticity modeling of AA2024-T3 aluminum alloy defined as the α-Al, θ-Al2Cu, and S-Al2CuMg phases based on real metallographic image. *Materials Research Express*, 2021. 8(10): p. 106521.

[4] Karimzadeh, A., M. Ayatollahi, and M. Alizadeh, Finite element simulation of nano-indentation experiment on aluminum 1100. *Computational Materials Science*, 2014. 81: p. 595-600.

[5] Rice, J.R., Inelastic constitutive relations for solids: an internal-variable theory and its application to metal plasticity. *Journal of the Mechanics and Physics of Solids*, 1971. 19(6): p. 433-455.

[6] Peirce, D., R.J. Asaro, and A. Needleman, Material rate dependence and localized deformation in crystalline solids. *Acta metallurgica*, 1983. 31(12): p. 1951-1976.

[7] Asaro, R.J., Crystal plasticity. 1983.

[8] Peirce, D., R. Asaro, and A. Needleman, An analysis of nonuniform and localized deformation in ductile single crystals. *Acta metallurgica*, 1982. 30(6): p. 1087-1119.

[9] Evans, J.A., et al., Determining elastic anisotropy of textured polycrystals using resonant ultrasound spectroscopy. *Journal of Materials Science*, 2021. 56(16): p. 10053-10073.

[10] Lim, H., et al., Investigating mesh sensitivity and polycrystalline RVEs in crystal plasticity finite element simulations. *International Journal of Plasticity*, 2019. 121: p. 101-115.

[11] Liu, M., et al., A crystal plasticity study of the effect of friction on the evolution of texture and mechanical behaviour in the nano-indentation of an aluminium single crystal. *Computational materials science*, 2014. 81: p. 30-38.

[12] Karthik, V., et al., Finite element analysis of spherical indentation to study pile-up/sink-in phenomena in steels and experimental validation. *International Journal of Mechanical Sciences*, 2012. 54(1): p. 74-83.

[13] Howe, S. and C. Elbaum, The relation between the plastic deformation of aluminium single crystals and polycrystals. *Philosophical Magazine*, 1961. 6(61): p. 37-48.